The Plant Cell, Vol. 25: 1609–1624, May 2013, www.plantcell.org

MIXTA-Like Transcription Factors and WAX INDUCER1/SHINE1 Coordinately Regulate Cuticle Development in *Arabidopsis* and *Torenia fournieri*[C][W]

Yoshimi Oshima,[a] Masahito Shikata,[b,1] Tomotsugu Koyama,[a,2] Norihiro Ohtsubo,[b] Nobutaka Mitsuda,[a,3] and Masaru Ohme-Takagi[a]

[a] Bioproduction Research Institute, National Institute of Advanced Industrial Science and Technology, Higashi 1-1-1, Tsukuba 305-8562, Japan

[b] National Institute of Floricultural Science, National Agriculture and Food Research Organization, Tsukuba, Ibaraki 305-8519, Japan

The waxy plant cuticle protects cells from dehydration, repels pathogen attack, and prevents organ fusion during development. The transcription factor WAX INDUCER1/SHINE1 (WIN1/SHN1) regulates the biosynthesis of waxy substances in *Arabidopsis thaliana*. Here, we show that the MIXTA-like MYB transcription factors MYB106 and MYB16, which regulate epidermal cell morphology, also regulate cuticle development coordinately with WIN1/SHN1 in *Arabidopsis* and *Torenia fournieri*. Expression of a MYB106 chimeric repressor fusion (*35S:MYB106-SRDX*) and knockout/down of *MYB106* and *MYB16* induced cuticle deficiencies characterized by organ adhesion and reduction of epicuticular wax crystals and cutin nanoridges. A similar organ fusion phenotype was produced by expression of a WIN1/SHN1 chimeric repressor. Conversely, the dominant active form of MYB106 (*35S:MYB106-VP16*) induced ectopic production of cutin nanoridges and increased expression of *WIN1/SHN1* and wax biosynthetic genes. Microarray experiments revealed that MYB106 and WIN1/SHN1 regulate similar sets of genes, predominantly those involved in wax and cutin biosynthesis. Furthermore, *WIN1/SHN1* expression was induced by MYB106-VP16 and repressed by MYB106-SRDX. These results indicate that the regulatory cascade of MIXTA-like proteins and WIN1/SHN1 coordinately regulate cutin biosynthesis and wax accumulation. This study reveals an additional key aspect of MIXTA-like protein function and suggests a unique relationship between cuticle development and epidermal cell differentiation.

INTRODUCTION

The plant cuticle, which covers the surface of epidermal cells, consists of the lipophilic polymer cutin and cuticular waxes, which are synthesized from long-chain fatty acids. The cuticle is secreted from epidermal cells to the outside of the cell wall and serves to attract pollinators, to protect plants from dehydration, pathogen, and insect attacks, and to prevent organ fusion. Wax and cutin composition, secretion, and synthesis are modulated during cell expansion (Suh et al., 2005) and vary in different tissues (Li et al., 2007; Li-Beisson et al., 2009). Many mutants defective in wax or cutin biosynthesis have been reported, including mutants of genes required for the elongation of very-long-chain fatty acids and mutants of genes required for cutin monomer biosynthesis; these mutants exhibit permeable cuticles, loss of epicuticular wax, and/or loss of cutin nanoridges on the surface of flowers (Jenks et al., 1995; Tanaka et al., 2004; Li-Beisson et al., 2009).

In addition to the known biosynthetic mutants, several transcription factors (TFs) have been shown to regulate cuticle biosynthesis. The most intensively studied TFs involved in cuticle development are WAX INDUCER1 (WIN1)/SHINE1 (SHN1) and its phylogenetic neighbors in the AP2/ERF family. *WIN1/SHN1* gain-of-function mutants from *Arabidopsis thaliana* and barley (*Hordeum vulgare*) have been reported (Aharoni et al., 2004; Taketa et al., 2008). The *Arabidopsis shine* gain-of-function mutant and plants overexpressing *WIN1/SHN1*, *SHN2*, or *SHN3* have increased accumulation of epidermal wax, to levels severalfold higher than in the wild type, ectopic wax crystals in leaves, and increased expression of genes involved in wax biosynthesis, including *ECERIFERUM1* (*CER1*), *3-KETOACYL-COA SYNTHASE1* (*KCS1*), and *CER2* (Aharoni et al., 2004; Broun et al., 2004). Kannangara et al. (2007) reported that cutin was also increased in plants overexpressing *WIN1/SHN1*. After induction of *WIN1/SHN1* expression, the expression of cutin biosynthesis genes was induced, followed by the induction of wax biosynthesis genes (Kannangara et al., 2007). Recently, loss-of-function analysis using artificial microRNAs revealed that formation of nanoridges, petal surface structures that are composed of cutin, are redundantly regulated by WIN/SHNs (Shi et al., 2011).

Some MYB TFs are also involved in the regulation of cuticle development. The expression of these genes is affected by environmental stresses and/or developmental stages. For instance, two closely related stress-responsive MYB TFs, MYB30 and MYB96, activate the biosynthesis of very-long-chain fatty acids (VLCFAs). Overexpression of these genes induced the hyperaccumulation of epidermal wax (Raffaele et al.,

[1] Current address: Division of Plant Sciences, National Institute of Agrobiological Sciences, Tsukuba, Ibaraki 305-8602, Japan.
[2] Current address: Suntory Foundation for Life Sciences, Bioorganic Research Institute, Wakayamadai, Shimamoto, Osaka 618-8503, Japan.
[3] Address correspondence to nobutaka.mitsuda@aist.go.jp.
The author responsible for distribution of materials integral to the findings presented in this article in accordance with the policy described in the Instructions for Authors (www.plantcell.org) is: Nobutaka Mitsuda (nobutaka.mitsuda@aist.go.jp).
[C] Some figures in this article are displayed in color online but in black and white in the print edition.
[W] Online version contains Web-only data.
www.plantcell.org/cgi/doi/10.1105/tpc.113.110783

2008; Seo et al., 2011). MYB41, which is expressed in response to salt, drought, abscisic acid, and cold stresses, regulates cell wall modification, cuticle metabolism (Cominelli et al., 2008), and short-term expression of salt-responsive genes (Lippold et al., 2009). Constitutive expression of *MYB41* made the leaf surface permeable (Cominelli et al., 2008). Most homeodomain-leucine zipper (HD-ZIP) group IV TFs, which are specifically expressed in epidermal cells, also regulate the expression of genes related to cuticle development, such as *FIDDLEHEAD* (*FDH*) (Abe et al., 2001). *OUTER CELL LAYER1* from maize (*Zea mays*) also directly

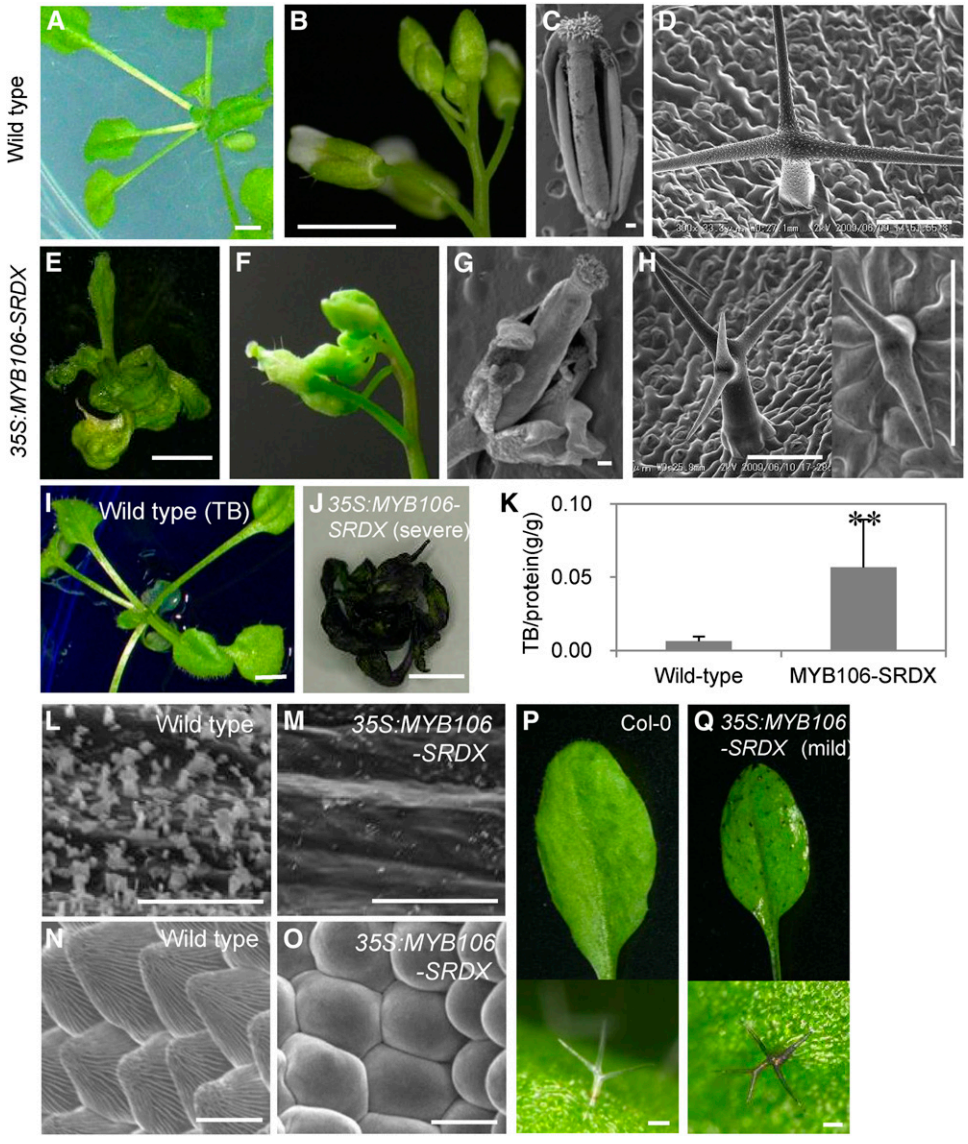

Figure 1. Phenotypes of 35S:MYB106-SRDX in *Arabidopsis*.

(A) and **(B)** Leaves **(A)** and floral buds **(B)** of the wild-type plant.
(C) and **(D)** Scanning electron micrograph of flower **(C)** and trichome **(D)** of wild-type *Arabidopsis*.
(E) and **(F)** Fused leaves **(E)** and floral buds **(F)** of a 5-week-old *35S:MYB106-SRDX* plant.
(G) and **(H)** Flower **(G)** and Trichome **(H)** of *35S:MYB106-SRDX Arabidopsis* observed by scanning electron microscopy.
(I) and **(J)** Wild-type **(I)** and severe-phenotype line of *35S:MYB106-SRDX* **(J)** plants stained with TB.
(K) TB uptake per gram protein. Error bars represent SE ($n = 8$). Double asterisks represent $P < 0.01$ by Welch's *t* test.
(L) to **(O)** Surface of stem (**[L]** and **[M]**) and petal (**[N]** and **[O]**) in the wild type (**[L]** and **[N]**) and *35S:MYB106-SRDX Arabidopsis* (**[M]** and **[O]**) observed by scanning electron microscopy.
(P) and **(Q)** Wild-type **(P)** and mild-phenotype line of *35S:MYB106-SRDX* **(Q)** *Arabidopsis* stained with TB. Bottom panels show magnified trichome images. Col-0, Columbia-0.
Bars = 2 mm in **(A)**, **(B)**, **(E)**, **(I)**, and **(J)**, 100 μm in **(C)**, **(D)**, **(G)**, **(H)**, **(P)**, and **(Q)**, and 10 μm in **(L)** to **(O)**.

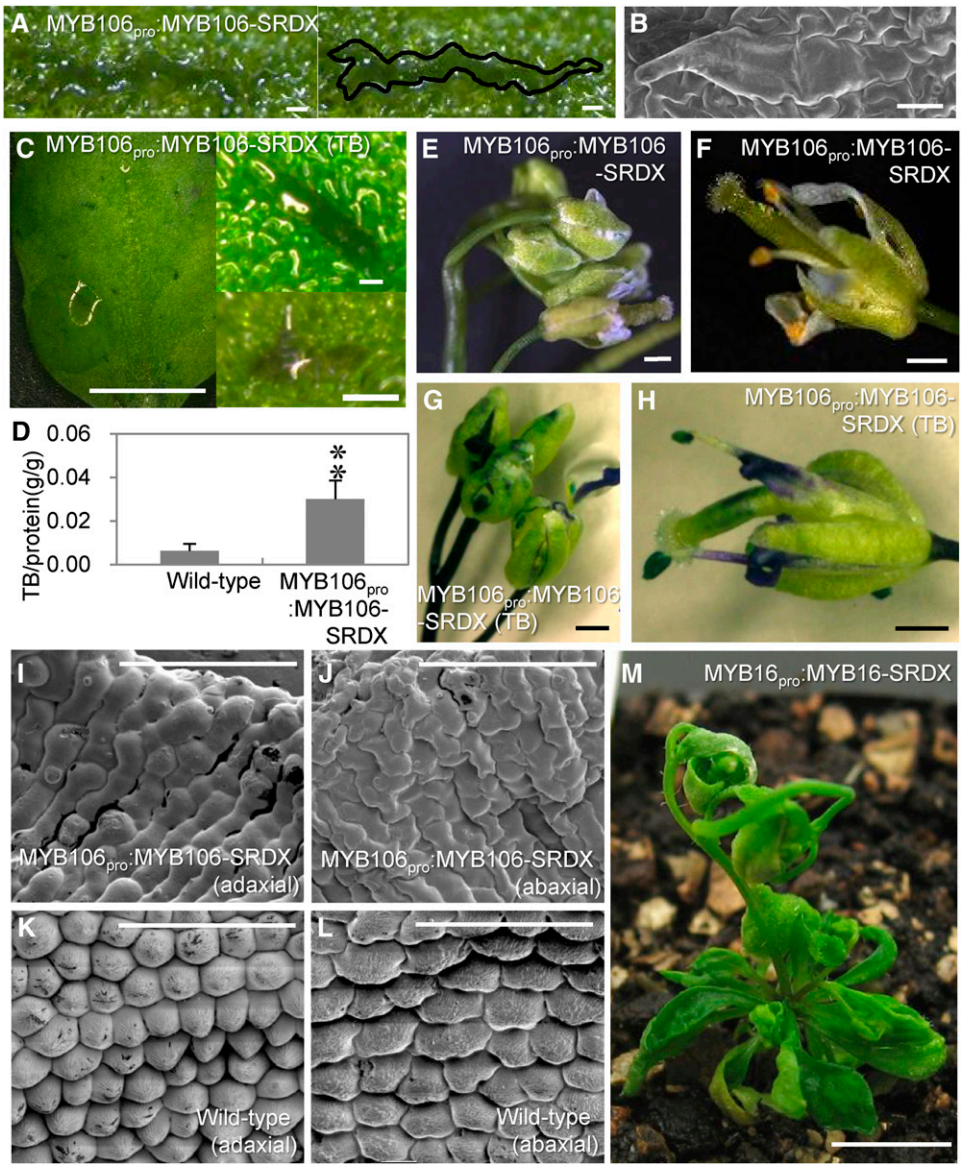

Figure 2. Morphological Changes and Cuticle Permeability in Transgenic *Arabidopsis* Expressing Chimeric Repressors of MIXTA-Like MYBs Driven by Their Native Promoters.

(A) and **(B)** Flatted trichome in the rosette leaf of *MYB106$_{pro}$:MYB106-SRDX Arabidopsis* **(A)** and its scanning electron microscopy observation **(B)**. The trichome is outlined with a black line in the right panel of **(A)**.

(C) A rosette leaf of a *MYB106$_{pro}$:MYB106-SRDX* plant stained with TB. A completely flatted trichome and a partly outgrown trichome are enlarged in the right panels.

(D) TB uptake per gram protein. Error bars represent SE (n = 8). Double asterisks represent $P < 0.01$ by Welch's t test.

(E) to **(H)** Fused buds (**[E]** and **[G]**) and flowers (**[F]** and **[H]**) of *MYB106$_{pro}$:MYB106-SRDX* plants, stained by TB (**[G]** and **[H]**).

(I) to **(L)** Surface of petals of *MYB106$_{pro}$:MYB106-SRDX* (**[I]** and **[J]**) and wild-type *Arabidopsis* (**[K]** and **[L]**) observed by scanning electron microscopy.

(M) Five-week-old *MYB16$_{pro}$:MYB16-SRDX* plant.

Bars = 50 μm in **(A)**, **(B)**, right panel of **(C)**, and **(I)** to **(L)**, 0.5 mm in **(E)** to **(H)**, and 5 mm in the left panel of **(C)** and **(M)**.

regulates the expression of *WHITE-BROWN COMPLEX11a* (Zm-*WBC11a*), an ortholog of At-*WBC11*, which is involved in the transport of wax and cutin (Javelle et al., 2010).

Subgroup-9 R2R3 MYB TFs, including snapdragon (*Antirrhinum majus*) *MIXTA*, were reported to be required for the development of petal trichomes and for formation of the conical shape of petal epidermal cells. Mutation of *MIXTA* or petunia (*Petunia hybrida*) *MYB1* prevents anticlinal growth of petal epidermal cells, resulting in altered intensity of petal color (Noda et al., 1994; Glover et al., 1998; Jaffé et al., 2007; Baumann et al., 2007). Another snapdragon MIXTA-like gene, *MYBML1*, which is expressed in specialized petal trichomes, induced ectopic differentiation of trichomes on carpels when it was overexpressed (Perez-Rodriguez et al., 2005). The *Arabidopsis noeck* (*nok*) mutant, which has a mutation in *NOK*/*MYB106*, exhibited overbranched trichomes, suggesting that NOK/MYB106 negatively regulates trichome branch formation (Folkers et al., 1997; Jakoby et al., 2008). The phenotypic and transcriptome analysis of *glabra3-shapeshifter nok* double mutants revealed that NOK/MYB106 regulates early morphogenic events of trichome formation (Gilding and Marks, 2010). These reports suggest the involvement of MIXTA-like MYBs in the specialization of epidermal cell shape.

In this study, we show that the MIXTA-like *Arabidopsis* genes *NOK*/*MYB106* and *MYB16* participate in the regulation of cuticle biosynthesis, partially cooperating with *WIN1*/*SHN1*, in *Arabidopsis* and *Torenia fournieri*. Here, we propose another important function of MIXTA-like genes, in addition to their role in epidermal cell differentiation, and explore the regulatory network of MIXTA-like MYBs and WIN1/SHN1.

RESULTS

Constitutive Expression of MIXTA-Like Genes with SRDX-Induced Severe Defect in Cuticle Development

Previously, we selected 50 TFs that likely participate in the regulation of organ development and/or cell differentiation; to examine their functions, we prepared independent *Arabidopsis* transgenic lines that express the chimeric repressor for each of these TFs (Shikata et al., 2011). Each chimeric repressor construct was prepared by fusing the TF gene with the SRDX repression domain (Leu-Asp-Leu-Asp-Leu-Glu-Leu-Arg-Leu-Gly-Phe-Ala; Hiratsu et al., 2003). The chimeric repressor for a specific TF should repress the target genes of that TF even in the presence of the endogenous TF itself or other TFs activating the same targets. Therefore, the chimeric repressor will induce a phenotype similar to the phenotype of a loss-of-function mutant of a transcriptional activator. If functionally redundant genes activate the same target, the chimeric repressor will phenocopy the multiple mutant phenotype. In examining the chimeric repressor lines, we found that plants expressing a chimeric repressor for MYB106, driven by the cauliflower mosaic virus 35S promoter (*35S*:*MYB106-SRDX*), showed adhesions between leaves and between buds, overbranched, and smooth-surfaced trichomes (Figures 1A to 1H). Among 31 T1 transgenic plants, 30 plants showed these phenotypes to a varying extent (see Supplemental Table 1 online). The overbranched trichome phenotype is also observed in *nok* mutants, which lack *MYB106* function (Folkers et al., 1997; Jakoby et al., 2008). MYB106-SRDX also induced immature-appearing trichomes with fewer branches (Figure 1H; see Supplemental Table 2 online). The adhesion phenotypes seen in *35S:MYB106-SRDX* plants are similar to the phenotypes of

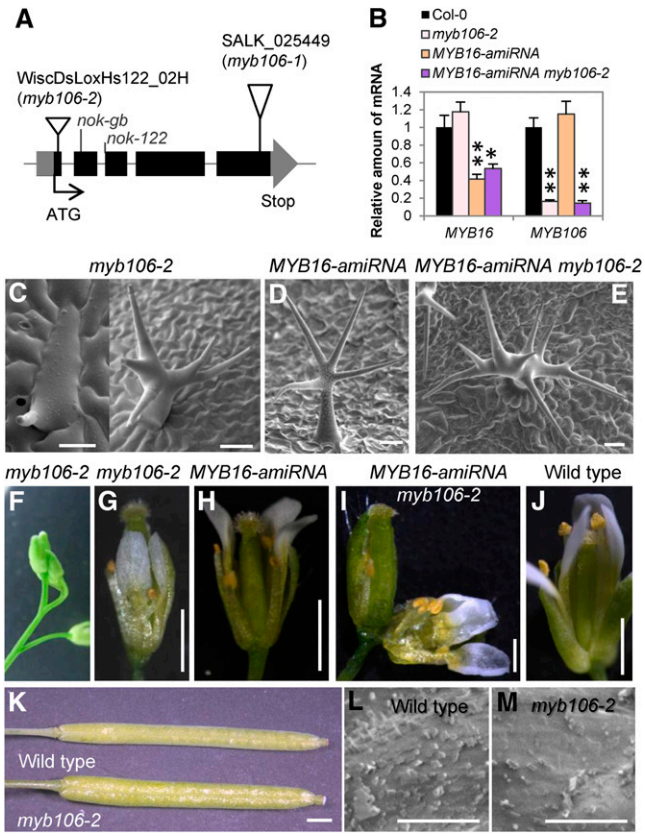

Figure 3. Phenotypes of the *myb106-2* Mutant, *MYB16-amiRNA* Plant, and *MYB16-amiRNA myb106-2* Double Knockout/down in *Arabidopsis*.

(A) Structure of the *MYB106* gene and the position of mutation or T-DNA insertion. T-DNA insertion and mutation of each mutant are shown. Black boxes, a gray box, and a gray arrow indicate coding region, 5′ untranslated region, and 3′ untranslated region, respectively.

(B) qRT-PCR analysis of expression of *MYB16* and *MYB106* in buds of wild-type, *myb106-2*, *MYB16-amiRNA*, and *MYB16-amiRNA myb106-2* plants. Expression level in the wild type is set to 1. Error bars represent SE (n = 3 or 4). Single and double asterisks represent $P < 0.05$ and $P < 0.01$ by Welch's t test, respectively. Col-0, Columbia-0.

(C) to **(E)** Trichomes in the rosette leaves of *myb106-2* **(C)**, *MYB16-amiRNA* **(D)**, and *MYB16-amiRNA myb106-2* **(E)** plants observed by scanning electron microscopy.

(F) to **(J)** Fused buds **(F)** and flowers (**[G]** to **[J]**) of *myb106-2* (**[F]** and **[G]**), *MYB16-amiRNA* **(H)**, *MYB16-amiRNA myb106-2* **(I)**, and wild-type **(J)** plants.

(K) Silique of the wild type and *myb106-2*.

(L) and **(M)** Surface of silique in the wild type **(L)** and *myb106-2* **(M)** observed by scanning electron microscopy.

Bars = 10 μm in **(L)** and **(M)**, 50 μm in **(C)** to **(E)**, and 1 mm in **(G)** to **(K)**.

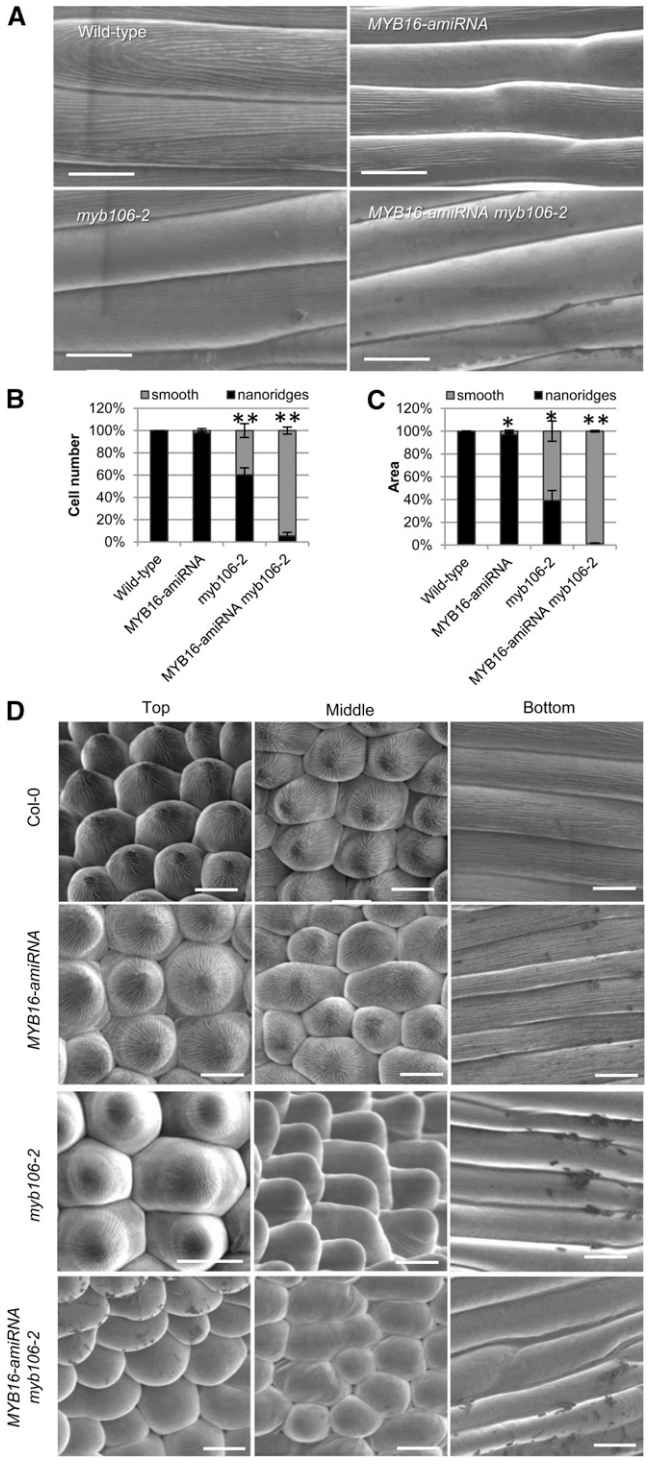

Figure 4. Surface of Filaments and Petals in the *myb106-2* Mutant, *MYB16-amiRNA* Plant, and *MYB16-amiRNA myb106-2* Double Knockout/down Plant.

(A) Surface of filaments observed by scanning electron microscopy.
(B) and **(C)** Frequency of cells **(B)** and areas **(C)** with nanoridges or without nanoridges (smooth) in one side of each filament. Error bars represent SE ($n = 3$). A total of 110 to 227 cells for each filament were examined. Single and double asterisks represent $P < 0.05$ and $P < 0.01$ by Welch's *t* test, respectively.

mutants with cuticle defects (Yephremov et al., 1999; Wellesen et al., 2001; Bach et al., 2008; Panikashvili et al., 2009). To examine whether the adhesion phenotype results from a defect in surface cuticle, we used a toluidine blue (TB) test, in which plants with defective cuticle are stained with an aqueous dye that cannot penetrate plants with a normal cuticle (Tanaka et al., 2004). We found that large parts of the leaves of *35S:MYB106-SRDX* plants stained blue, having absorbed a substantial amount of TB (Figures 1I, 1J, and 1K). Because in *Arabidopsis* a severe *35S:MYB106-SRDX* phenotype resulted in lethality, we examined *35S:MYB106-SRDX* lines with a mild phenotype and found that they had reduced epicuticular wax crystals on the stem (Figures 1L and 1M) and no nanoridges on petals (Figures 1N and 1O). The outgrowth of petal epidermal cells was suppressed, reflecting MIXTA function (Figures 1N and 1O). Moreover, the top region and margin of sepals and anthers, and the leaf trichomes stained clearly with TB (Figures 1P to 1R; see Supplemental Figure 1 online). These results indicate that *35S:MYB106-SRDX Arabidopsis* are defective in cuticle formation. To investigate whether this molecular function of MIXTA-like proteins in cuticle formation is conserved among different plant species, we introduced the *35S:MYB106-SRDX* construct into *Torenia* and found that cuticle defects were induced as observed in *Arabidopsis* (see Supplemental Figures 1E and 1F online).

MYB106 belongs to MYB subgroup 9 and is similar to MYB16, MYB17, and the snapdragon MIXTA protein (Stracke et al., 2001). To examine functional redundancy among MIXTA-like genes, we compared microarray data along with developmental stages using AtGenExpress Visualization Tool (Schmid et al., 2005) and conserved protein motif using SALAD database (Mihara et al., 2008; see Supplemental Figure 2 and Supplemental Reference 1 online). These results indicate that expression pattern and protein motif composition of MYB106 gene/protein are much more similar to those of MYB16 rather than MYB17. The phylogenetic tree based on protein motif composition strongly suggests that MYB106 and MYB16 were recently separated in evolutional history because almost the same conserved protein motifs are shared (see Supplemental Figure 2C online), suggesting that *MYB16* is a paralogous gene of *MYB106*. In addition, MYB17 was reported to play a role in the transition of meristem identity (Pastore et al., 2011). The transgenic plants that expressed the chimeric repressors of *MYB16* (*35S:MYB16-SRDX*) exhibited similar phenotypes to plants expressing *35S:MYB106-SRDX* (see Supplemental Figure 3 online), which supported our hypothesis.

Promoter Activities of MIXTA-Like Genes Are Largely Overlapping, with Some Distinct Profiles

To validate the above hypothesis further, we performed promoter-reporter experiments with the MIXTA-like genes and

(D) The surface of petals observed by scanning electron microscopy. Col-0, Columbia-0.
Bars = 10 μm.

found that the promoter activity of *MYB106* was relatively high in young trichomes, stems, at the boundaries between stems and pedicels, in flowers, and in the dehiscence zone (see Supplemental Figures 4A to 4E and 5 online), as reported previously (Jakoby et al., 2008). *MYB16* promoter activity was evident in stem, buds, trichomes, epidermis, and mesophyll cells of young leaves (see Supplemental Figures 4F to 4H and 5 online). Detailed observation of flowers revealed that *MYB16* and *MYB106* appear to be redundantly expressed in young petals, but the expression of *MYB16* in petals disappeared slightly earlier (see Supplemental Figure 5 online). These two genes also appeared to be expressed in young carpel, sepal, and stamen tissue. *MYB106* appeared to be expressed until stage 12 in long filament, whereas expression of *MYB16* in filaments continued until stage 13 (see Supplemental Figure 5 online). These data indicate that the expression of *MYB16* and *MYB106* overlapped in most but not all tissues.

Expression of MIXTA-Like Genes with SRDX Driven by Their Own Promoters Induced Similar Phenotypes

To analyze the biological functions of MIXTA-like MYBs in more detail, we prepared transgenic plants that expressed each chimeric repressor under the control of its own promoter (*MYB106*$_{pro}$:*MYB106-SRDX* and *MYB16*$_{pro}$:*MYB16-SRDX*). We found that

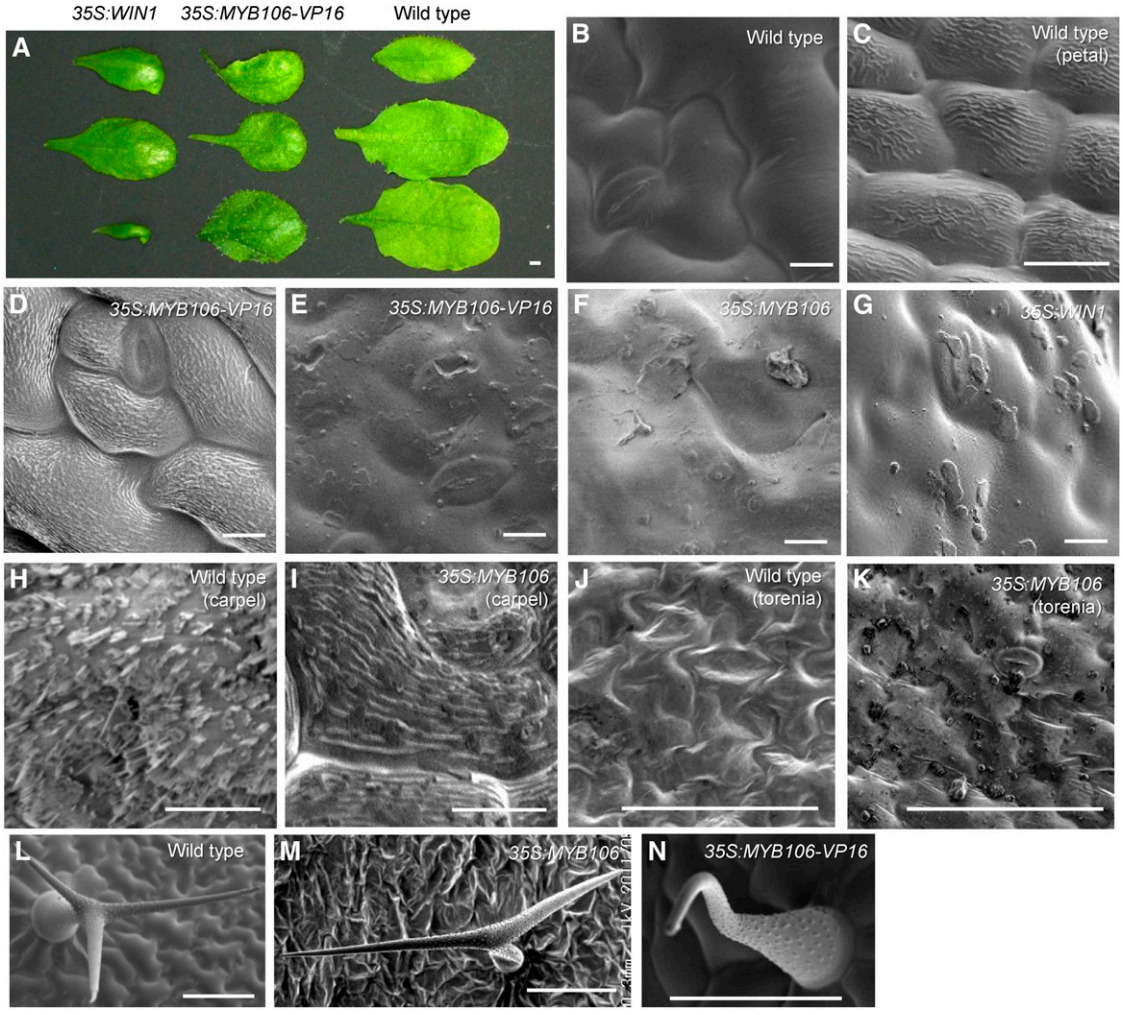

Figure 5. Ectopic Formation of Nanoridges and Wax Crystals in *35S*:*MYB106-VP16* and *35S*:*MYB106* Plants.

(A) Rosette leaves of wild-type, *35S*:*MYB106-VP16*, and *35S*:*WIN1* plants. Three leaves cut from different positions and different T1 lines.
(B) to **(I)** Surface of rosette leaves (**[B]**, **[D]**, to **[G]**), petals **(C)**, and carpels (**[H]** and **[I]**) in wild-type (**[B]**, **[C]**, and **[H]**), *35S*:*MYB106-VP16* (**[D]** and **[E]**), *35S*:*MYB106* (**[F]** and **[I]**), and *35S*:*WIN1* **(G)** *Arabidopsis* observed by scanning electron microscopy. Replica experiments showed similar results to **(B)** to **(E)** and **(G)**.
(J) and **(K)** Surface of leaves in wild-type **(J)** and *35S*:*MYB106* **(K)** *Torenia* observed by scanning electron microscopy.
(L) to **(N)** Trichomes in the wild type **(L)**, *35S*:*MYB106* **(M)**, and *35S*:*MYB106-VP16* **(N)** observed by scanning electron microscopy.
Bars = 1 mm in **(A)** and 0.1mm in **(B)** to **(N)**.
[See online article for color version of this figure.]

MYB106$_{pro}$:*MYB106-SRDX* plants exhibited flattened trichomes and fused flowers with narrow petals (Figures 2A, 2B, 2E, and 2F). Most outgrown trichomes were unbranched, and the total number of outgrown trichomes was reduced in *MYB106*$_{pro}$:*MYB106-SRDX* plants (see Supplemental Table 2 online). Flattened trichomes seem to be caused by defective trichome outgrowth. TB staining showed permeable cuticles in the flattened trichomes, petals, stamens, part of carpels and sepals, pedicels, and stems (Figures 2C, 2D, 2G, and 2H), while flowers and pedicels of wild-type plants were not stained (see Supplemental Figure 1A online). The petal epidermal cells of *MYB106*$_{pro}$:*MYB106-SRDX* plants were flattened and slender and lacked nanoridges (Figures 2I to 2L). Among 28 T1 transgenic plants, 16 plants showed the above-described phenotypes to a varying extent (see Supplemental Table 1 online). The petal and trichome phenotypes were more severe than those of *35S*:*MYB106-SRDX* plants. This is probably due to stronger activity of the *MYB106* promoter in petals and trichomes or may be due to lethality of *35S*:*MYB106-SRDX* plants with more severe phenotypes. In addition, *MYB16*$_{pro}$:*MYB16-SRDX* plants showed adhesion of flowers and leaves (Figure 2M). These data indicate that MYB106 and MYB16 act on organ separation and cuticle development in the tissues where they are normally expressed and that almost all of the phenotypes observed in the *35S*:*MYB106/16-SRDX* plants were partly reproduced either in *MYB106*$_{pro}$:*MYB106-SRDX* or *MYB16*$_{pro}$:*MYB16-SRDX* plants.

Knockdown/out of MIXTA-Like Genes Showed Defects in Cuticle Development

A T-DNA tagged line of *MYB106* (*myb106-1*) was previously shown to have overbranched trichomes (Jakoby et al., 2008), but no T-DNA–tagged line was available for *MYB16*. To analyze whether knockdown lines of MIXTA-like MYBs exhibit defects in cuticle formation, we transformed the *MYB106*-RNAi (for RNA interference) construct (*35S*:*MYB106-RNAi*) into wild-type *Arabidopsis* and found that the plants with severely or moderately reduced expression of *MYB106* and *MYB16*, respectively, exhibited a weak but similar phenotype to *35S*:*MYB106-SRDX* plants, including organ adhesion inside flowers, TB staining on the edges of sepals and petals, and trichome defects (see Supplemental Figure 6 online). Among 46 T1 transgenic *35S*:*MYB106-RNAi* plants, 38 plants showed a similar phenotype to *35S*:*MYB106-SRDX* plants to a varying extent (see Supplemental Table 1 online), suggesting that *35S*:*MYB106-SRDX* plants show accurate loss-of-function phenotypes. To analyze the specific function of each gene in cuticle development, we examined single knockout lines for *MYB106* and a single knockdown line for *MYB16*. In addition to *myb106-1* (SALK_025449), we analyzed *myb106-2* (WiscDsLoxHs 122_02H), in which the T-DNA is inserted close to the start codon (Figure 3A). Less-branched or overbranched trichomes were more frequently observed in *myb106-2* than in *myb106-1*, suggesting that *myb106-2* is more severe than *myb106-1* (see Supplemental Table 2 online). The trichome cell surface was smooth without papillae and, therefore, similar to that in *35S*:*MYB106-SRDX* and *MYB106*$_{pro}$:*MYB106-SRDX* plants (Figure 3C). To generate *MYB16* single knockdown and *MYB16* and *MYB106* double knockout/down plants, an artificial microRNA (amiRNA) construct of MYB16 (*MYB16-amiRNA*) was introduced into the wild type and *myb106-2*. The expression of *MYB16* in *MYB16-amiRNA* and *MYB16-amiRNA myb106-2* plants was suppressed to approximately half, while the expression of *MYB106* in *MYB16-amiRNA* plants was similar to the wild type (Figure 3B). In *MYB16-amiRNA* plants, the trichome branching number was slightly increased but the papillae still looked normal (Figure 3D; see Supplemental Table 2 online). In *MYB16-amiRNA myb106-2* plants, the trichome branching number was dramatically increased compared with both *MYB16-amiRNA* and *myb106-2* plants, and papillae on trichomes were similar to *myb106-2* plants (Figure 3E; see Supplemental Table 2 online). These results suggest

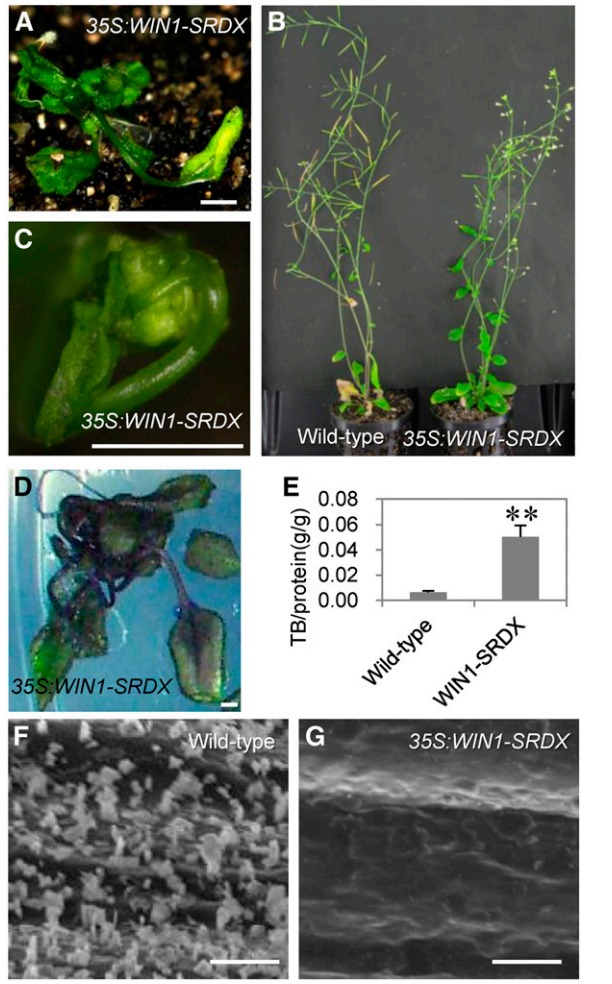

Figure 6. Phenotypes of Plants Expressing the WIN1/SHN1 Chimeric Repressor.

(A) to **(C)** Fused leaves **(A)**, entire appearance **(B)**, and fused bud **(C)** of *35S*:*WIN1-SRDX* plant.

(D) *35S*:*WIN1-SRDX* seedling stained with TB.

(E) TB uptake per gram protein. Error bars represent SE (n = 8). Double asterisks represent $P < 0.01$ by Welch's t test.

(F) and **(G)** Surface of stem of wild-type **(F)** and *35S*:*WIN1-SRDX* **(G)** *Arabidopsis* observed by scanning electron microscopy.

Bars = 5 mm in **(A)** and **(D)** and 50 μm in **(C)**, **(F)**, and **(G)**.

that *MYB16* is involved in termination of branching, whereas *MYB106* is involved in papillae formation, initiation of outgrowth, and termination of branching during trichome development. By contrast, the buds and the flowers of *myb106-2* plants were fused and the stamens of *MYB16-amiRNA* flowers were slightly short (Figures 3F to 3H). *MYB16-amiRNA myb106-2* plants showed more pronounced phenotypes in which petals were stacked in an unopened flower and stamens were short (Figure 3I). We observed the surface of stamen filaments by scanning electron microscopy and found that nanoridges were not formed in 3% of the area of *MYB16-amiRNA* filaments, in the bottom part of *myb106-2* filaments, and in the whole *MYB16-amiRNA myb106-2* filaments (Figures 4A to 4C). These data indicate that *MYB16* and *MYB106* regulate nanoridge formation in filaments. In addition, reduction of nanoridge formation and defects of cell outgrowth in *myb106-2* petals were enhanced in *MYB16-amiRNA myb106-2* plants, suggesting redundant function of the MIXTA-like genes in petal cell morphogenesis and supporting the results of chimeric repressor experiments (Figure 4D). In addition, the *myb106-2* plants produced siliques that were glossy due to the lack of white wax crystals on their surface, indicating a role for *MYB106* in wax production (Figures 3K to 3M).

MYB106 Can Induce Ectopic Formation of Nanoridges and Waxy Cuticle Substances

To analyze whether MIXTA-like MYBs have the ability to induce biosynthesis of wax and related substances, we generated plants that expressed the dominant active form of MYB106, in which the coding region of MYB106 was fused with the VP16 activation domain from herpes simplex virus (*35S:MYB106-VP16*). We found that most of the *35S:MYB106-VP16* plants exhibited less-branched trichomes and slightly shiny leaves, opposite to the phenotypes of the *35S:MYB106-SRDX* plants (Figures 5A and 5L to 5N; Aharoni et al., 2004). Observation by scanning electron microscopy revealed that the nanoridges that usually develop on petal epidermis were ectopically produced on the leaves of *35S:MYB106-VP16* plants (Figures 5C and 5D). In addition, plate-like wax crystals occasionally accumulated on the leaves of *35S:MYB106-VP16* and *35S:WIN1/SHN1* plants, which were used as the positive control (Figures 5E and 5G). *35S:MYB106* plants, without the VP16 activation domain, also exhibited less-branched trichomes, increased nanoridges on petals, ectopic nanoridge formation on the carpel, and ectopic plate-like wax crystals on leaves when an efficient transcriptional terminator was employed for plasmid construction (Figures 5F and 5I). Also in *Torenia*, the *35S:MYB106* construct induced overaccumulation of wax crystals on the leaves (Figure 5K). These results indicate that MYB106 has the ability to induce ectopic formation of cutin nanoridges and epicuticular wax in aboveground organs.

Chimeric Repressors of WIN/SHNs Induced Severe Cuticle Defects and Morphological Changes

By analysis of triple knockdown lines, overexpression lines, and gain-of-function mutants, three WIN/SHN TFs belonging to the

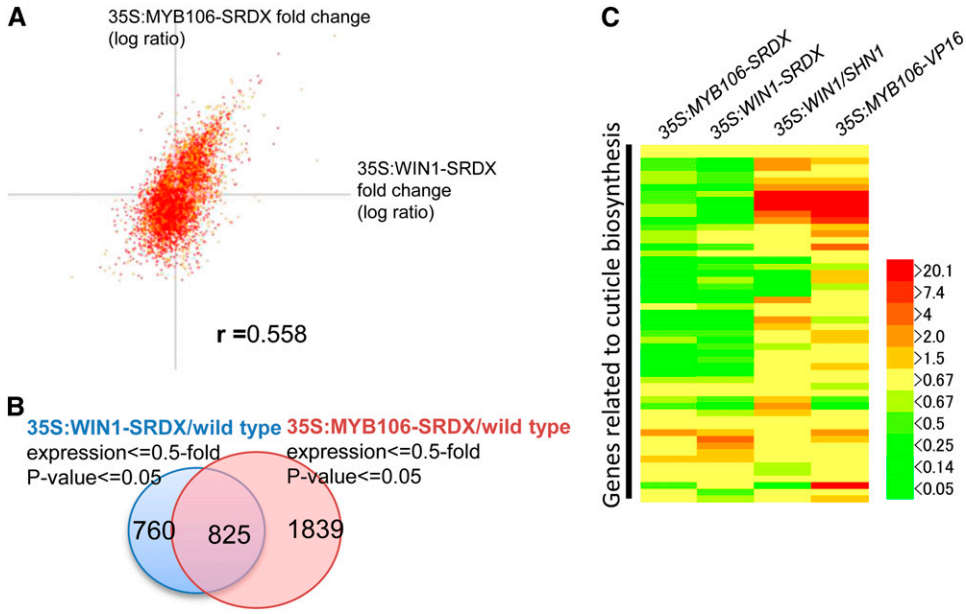

Figure 7. Transcriptome Analysis of *MYB106* and *WIN1/SHN1* Transgenic Plants.

(A) XY plot of fold change in *35S:WIN1-SRDX* and *35S:MYB106-SRDX* plants. Each dot indicates an individual probe in the microarray. *x* and *y* axes indicate log value of fold change in *35S:WIN1-SRDX* and *35S:MYB106-SRDX* plants, respectively.

(B) Venn diagram showing overlap of downregulated genes in *35S:MYB106-SRDX* and *35S:WIN1-SRDX* plants.

(C) Heat map showing expression of genes (fold change relative to the wild type) related to cuticle biosynthesis in *35S:MYB106-SRDX*, *35S:WIN1-SRDX*, *35S:WIN1*, and *35S:MYB106-VP16* plants.

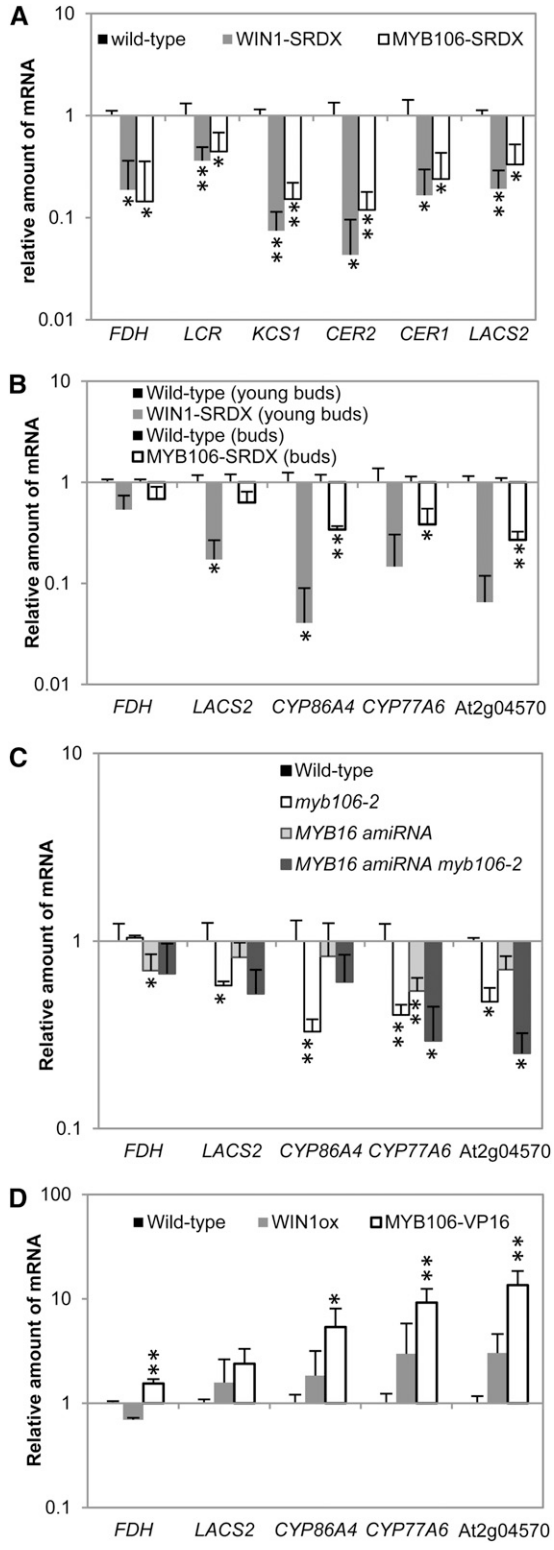

Figure 8. Expression of Cuticle-Related Genes in Transgenic Plants and Mutants.

(A) qRT-PCR analysis of expression of genes involved in cutin and wax biosynthesis in 3-week-old wild-type, *35S*:*MYB106-SRDX*, and *35S*:*WIN1-SRDX* plants. Expression level in the wild type is set as 1.

(B) qRT-PCR analysis of expression of genes involved in cutin and wax biosynthesis in buds of the wild type and *35S*:*MYB106-SRDX* and in young buds with a cauline leaf, as shown in Figure 6C, of wild-type and *35S*:*WIN1-SRDX* plants.

(C) qRT-PCR analysis of expression of genes involved in cutin and wax biosynthesis in buds of wild-type, *myb106-2*, *MYB16-amiRNA*, and *MYB16-amiRNA myb106-2* plants.

(D) qRT-PCR analysis of genes involved in cutin and wax biosynthesis in wild-type, 3-week-old *35S*:*MYB106-VP16* and *35S*:*WIN1* plants.

Error bars represent SD ($n = 4$ in **[A]** and **[B]**; $n = 3$ to 5 in **[C]**; $n = 3$ in **[D]**). Single and double asterisks indicate $P < 0.05$ and $P < 0.01$ in Welch's *t* test, respectively.

AP2/ERF TF family were previously shown to redundantly regulate the biosynthesis of cuticular wax and cutin (Aharoni et al., 2004; Broun et al., 2004; Kannangara et al., 2007; Shi et al., 2011). Compositional changes of cutin monomers and wax and morphological changes in petal epidermal cells were reported in the *WIN1/SHN1* knockdown lines (Kannangara et al., 2007; Shi et al., 2011). To analyze the biological function of *WIN/SHNs* in more detail, we generated transgenic *Arabidopsis* that expressed the *WIN1/SHN1* chimeric repressor (*35S*:*WIN1-SRDX*) and found that these plants exhibited much more dramatic phenotypes than those of the triple knockdown line, namely, adhesion of leaves, increased surface permeability, and reduction of epicuticular wax crystals, suggesting that the chimeric repressor overcame the genetic redundancy of *WIN/SHNs* (Figures 6A to 6E and 6G). Among 65 T1 transgenic plants, 52 plants showed the above-described phenotypes to a varying extent (see Supplemental Table 1 online). In addition, we also analyzed the function of *SHN3*, a homolog of *WIN1/SHN1*, and found that *35S*:*SHN3-SRDX* plants exhibited more severe flower phenotypes than *35S*:*WIN1-SRDX* plants: Bud and pedicel were fused, and the petal had no nanoridges (see Supplemental Figure 7 online). We also generated transgenic *Torenia* expressing *WIN1-SRDX* and found that this construct induced a permeable cuticle (see Supplemental Figure 7G online). These results suggest that WIN/SHNs have essential roles in both the development of cutin and wax and in organ separation.

MIXTA-Like *MYB*s Regulate the Expression of Genes for Cuticle Biosynthesis in a Similar Manner to *WIN/SHN*s

To investigate the role of MIXTA-like MYBs in cuticle development, we performed microarray experiments on *35S*:*MYB106-SRDX*, *35S*:*WIN1-SRDX*, *35S*:*MYB106-VP16*, and *35S*:*WIN1* plants. We found that the *35S*:*MYB106-SRDX* and *35S*:*WIN1-SRDX* plants have similar transcriptomes ($r = 0.558$ for all genes; Figure 7A). More than 50% of the genes downregulated in the *35S*:*WIN-SRDX* plants (fold change < 0.5 and P value < 0.05; false discovery rate [FDR] < 0.048, 1585 genes) are also downregulated (fold change < 0.5 and P value < 0.05; FDR < 0.0291, 2664 genes) in *35S*:*MYB106-SRDX* plants (Figure 7B). Genes involved in cuticle development, including fatty acid elongation and wax biosynthetic pathways, cutin biosynthesis, and lipid transport, were overrepresented among the genes downregulated in *35S*:*MYB106-*

SRDX and *35S*:*WIN1-SRDX* plants and were also overrepresented among the genes upregulated in *35S*:*MYB106-VP16* and *35S*:*WIN1* plants (Figure 7C; see Supplemental Tables 3 and 4 online).

Further detailed analyses using quantitative RT-PCR (qRT-PCR) revealed that the expression of *FDH* (Yephremov et al., 1999; Pruitt et al., 2000); *KCS1* (Todd et al., 1999); *CER1* and *CER2* (Jenks et al., 1995), which are required for wax accumulation; *LACERATA* (Wellesen et al., 2001) and *LONG-CHAIN ACYL-COA SYNTHETASE2* (Schnurr et al., 2004), which are involved in cutin biosynthesis, was reduced in both *35S*:

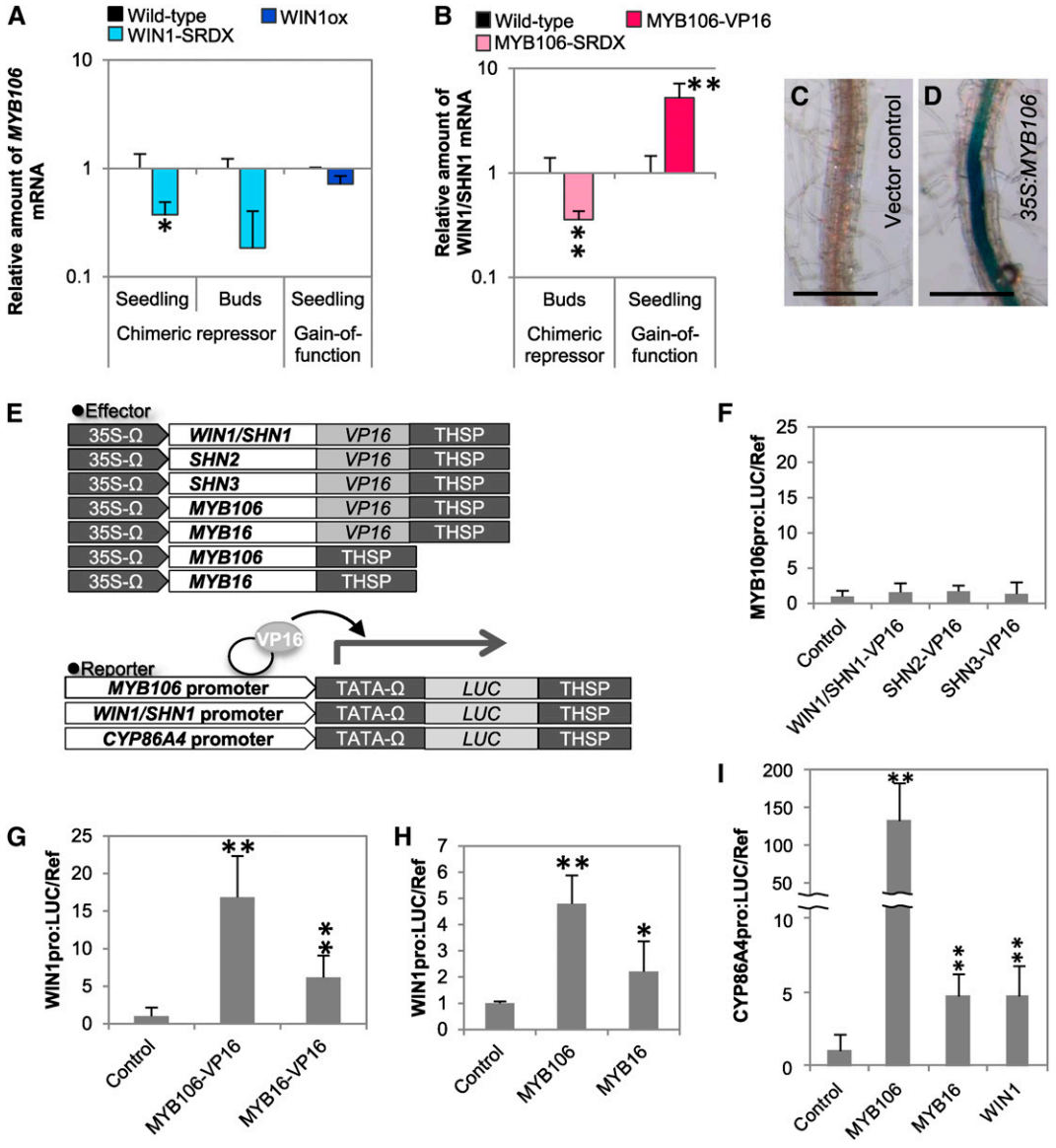

Figure 9. Regulatory Relationship between *WIN1/SHN1* and *MYB106*.

(A) and **(B)** qRT-PCR analysis of expression of *MYB106* **(A)** and *WIN1/SHN1* **(B)** in 3-week-old plants (seedling) and buds of wild-type, *35S*:*WIN1-SRDX*, *35S*:*MYB106-SRDX*, *35S*:*WIN1*, and *35S*:*MYB106-VP16* plants.

(C) and **(D)** GUS reporter activity (blue color) driven by the promoter of *WIN1/SHN1* in root of control **(C)** and *35S*:*MYB106* **(D)** plant.

(E) Schematic representation of effector and reporter constructs for transient gene expression analysis done in **(F)** to **(I)**. 35S, cauliflower mosaic virus 35S promoter; Ω, the translational enhancer sequence from *Tobacco mosaic virus*; THSP, *Arabidopsis HSP18.2* terminator; LUC, firefly luciferase.

(F) to **(I)** Transient gene expression analysis of the LUC reporter driven by *MYB106* **(F)**, *WIN1/SHN1* (**[G]** and **[H]**), and *CYP86A4* **(I)** promoters. The LUC activity obtained when empty vector or VAMP722VP16 effector (control; see Methods) was coexpressed was set to 1. *MYB106*, *MYB16*, *WIN1/SHN1*, *SHN2*, and *SHN3* fused with or without VP16 were used as effectors.

Error bars represent SD (n = 3 to 4 in **[A]** and **[B]**; n = 6 in **[F]** to **[I]**). Single and double asterisks indicate $P < 0.05$ and $P < 0.01$ in Welch's t test, respectively. Bars = 0.5 mm.

MYB106-SRDX and *35S*:*WIN1-SRDX* plants, suggesting that cuticular wax and cutin biosynthesis were downregulated in these lines (Figure 8A). The expression of cutin biosynthetic genes was downregulated in flowers of *35S*:*MYB106-SRDX* and *35S*:*WIN1-SRDX* plants (Figure 8B) and to a lesser extent in flowers of *myb106-2*, *MYB16-amiRNA*, and *MYB16-amiRNA myb106-2* plants (Figure 8C). Conversely, the expression of genes involving in the biosynthesis of wax and cutin was increased in *MYB106-VP16* plants and in *35S*:*WIN1* plants (Figure 8D), but the entire transcriptomes of these plants showed more differences than did *MYB106-SRDX* and *WIN1-SRDX* plants.

MIXTA-Like *MYB*s Act as Positive Regulators of *WIN1/SHN*s

As suggested by the microarray experiments described above, it is plausible that MYB106 and WIN1/SHN1 may act in a similar cascade for cuticle development. To investigate the relationship between *MYB106* and *WIN1/SHN1*, we performed RT-PCR experiments using seedlings, young buds sampled from a severe-phenotype line of *35S*:*WIN1-SRDX* plants in which young buds could not grow due to the fusion, and buds sampled from *35S*:*MYB106-SRDX*. We found the expression of *MYB106* was not induced by WIN1/SHN1 even though it was downregulated to some extent in *35S*:*WIN1-SRDX* plants (Figure 9A). In addition, the promoter activity of *MYB106* in transient expression assays using $MYB106_{pro}$:*LUC* was not induced by WIN1-VP16 (Figure 9F), suggesting that *MYB106* is not downstream of WIN/SHNs in the cascade.

By contrast, the expression of *WIN1/SHN*s appears to be regulated more precisely by MIXTA-like *MYB*s because the expression of *WIN1/SHN1* was apparently reduced in flowers of *35S*:*MYB106-SRDX* plants (Figure 9B). It should be noted that, in seedlings, we did not detect reduced expression of *WIN1/SHN1*, which was not expressed in the seedling stage (Broun et al., 2004). Moreover, MYB106, MYB106-VP16, and MYB16-VP16 also activated the *WIN1/SHN1* promoter (Figures 9D and 9G). In addition, mRNA expression of *WIN1/SHN1* was upregulated in *35S*:*MYB106-VP16* plants (Figure 9B), and *WIN1/SHN1* promoter activity was ectopically activated in *35S*:*MYB106* plants (Figure 9D). These results suggest that MYB106 acts as a positive regulator of *WIN1/SHN1*. Furthermore, MYB106 and MYB16 activate the promoter of *CYP86A4*, which was reported to be a putative direct target of WIN1/SHN1. However, activation of *CYP86A4* by MYB106 was 24-fold higher than the activation by WIN1/SHN1 (Figure 9I; Shi et al., 2011). This raises the possibility that MYB106 also has an important role in the regulation of *CYP86A4*. Our results indicate that MYB106 positively regulates *WIN1/SHN1* expression, but its function may not depend on WIN1/SHN1 completely.

DISCUSSION

In this study, we identified a chimeric repressor that induced an organ adhesion phenotype, which is often observed in mutants defective in cuticle biosynthesis or transport. Following up on that observation, we found that one of the MIXTA-like MYBs, MYB106, which regulates the morphology of epidermal cells (Jakoby et al., 2008; Gilding and Marks, 2010), is a positive regulator of cuticle development. Here, we discuss the roles of the MIXTA-like MYBs in cuticle development and the functional relationship between MYB106 and WIN1/SHN1 in the regulation of cuticle development.

The Role of MIXTA-Like MYBs in Cuticle Development in the Context of Epidermal Cell Differentiation

MIXTA-like MYBs from snapdragon, petunia, and *Arabidopsis* are known to regulate epidermal cell specification, morphology, and maturation; their roles in trichomes and petal epidermal cells are particularly well studied (Noda et al., 1994; Folkers et al., 1997; Glover et al., 1998; Baumann et al., 2007; Jaffé et al., 2007; Jakoby et al., 2008). Our results from chimeric repressor, activator, and knockout/down experiments also supported the above-mentioned functions of MIXTA-like MYBs (see Supplemental Tables 5 and 6 online). During the elongation of epidermal cells in an aerial organ, wax and cutin are loaded onto the outer surface of the epidermal cells (Suh et al., 2005). Cuticle composition varies in different organs, as exemplified by the petal, which has specialized cutin architecture, including structures such as nanoridges. Development of the cuticle occurs simultaneously with epidermal cell specialization. We found that MIXTA-like MYBs are common regulators of nanoridge formation and wax load as part of specialization of petal conical cells and cell elongation in filaments and siliques, which are made of nonoutgrown flat cells. Therefore, we propose a role for MIXTA-like MYBs in the

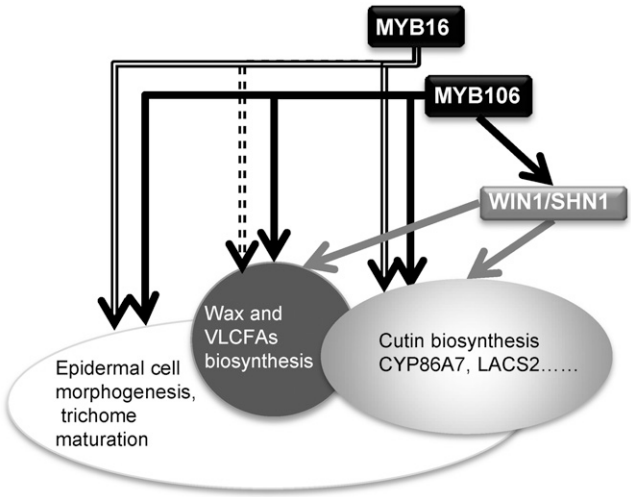

Figure 10. Regulation of Cuticle Development and Epidermal Differentiation by WIN1/SHN1 and MIXTA-like MYBs.

MYB16 regulates epidermal morphogenesis and cutin biosynthesis and likely regulates wax and VLCFA biosynthesis together with MYB106. MYB106 regulates epidermal cell morphogenesis, trichome maturation, wax and VLCFA biosynthesis, cutin biosynthesis, and *WIN1/SHN1* expression. WIN1/SHN1 was shown to regulate cutin and wax biosynthesis directly or indirectly (Kannangara et al., 2007; Shi et al., 2011). MYB106 regulates cutin biosynthesis via WIN1/SHN1-dependent and -independent pathways.

regulation of cuticle development during the differentiation of epidermal cells.

MIXTA-Like MYBs Are Global Regulators of Cuticular Substances

We demonstrated that MIXTA-like MYBs regulate biosynthesis of cutin nanoridges and wax accumulation by promoting the expression of related genes, based on the results of loss-of-function and gain-of-function analyses of *MYB106* and *MYB16*. In addition, the expression pattern and promoter analysis of each MIXTA-like *MYB* gene suggested that they are expressed in stems and pedicels, where wax is actively produced. Several *Arabidopsis* mutants defective in cutin accumulation exhibit a similar phenotype to loss-of-function mutants of MIXTA-like MYBs. For instance, mutation of *DEFECTIVE IN CUTICULAR RIDGES*, which encodes a soluble diacylglycerol acyltransferase required for cutin polyester formation, induces organ fusion in leaves, flowers, and seeds and changes in the decoration of petal conical cells (Panikashvili et al., 2009; Rani et al., 2010). The CYP86A8 defective mutant (*lcr*), which fails to catalyze ω-hydroxylation of fatty acids ranging from C12 to C18:1, also exhibits postgenital fusion in inflorescences and strong leaf fusion (Wellesen et al., 2001). Our loss- and gain-of-function analysis of *MYB106* and *MYB16* revealed that they regulate the expression of these cutin biosynthesis genes. In addition, the organ fusion and permeable cuticle phenotypes that were observed in *35S:MYB106-SRDX* plants were also observed in mutants of the VLCFA biosynthetic genes *FDH*, *COA CARBOXYLASE1*, and *PASTICCINO2* (*PAS2*), which encode a 3-ketoacyl-CoA synthase gene, the main enzyme in cytosolic malonyl-CoA synthesis, and 3-hydroxy-acyl-CoA dehydratase, respectively (Lolle et al., 1992, 1997; Yephremov et al., 1999; Bach et al., 2008; Lü et al., 2011). The expression of these enzymatic genes was also regulated by MYB106. *PAS1* and *PAS2*, which were identified as mutants of cell proliferation, are involved in the biosynthesis of VLCFA and its derivatives, including sphingolipids, which are required for polar auxin transport and tissue patterning during plant development and for cell plate formation during cytokinesis (Roudier et al., 2010; Bach et al., 2011). Although the expression of *PAS1* was not affected by MYB106 expression modification, the expression of *PAS2*, *BETA-KETOACYL REDUCTASE1*, and *CER10*, which encode enzymes associated with PAS1 (Roudier et al., 2010), was reduced (0.5-, 0.45-, and 0.57-fold of the wild type) in the *MYB106-SRDX* plants and was increased (2.36-, 1.43-, and 1.11-fold of the wild type) in the *MYB106-VP16* plants, respectively, in our microarray data. MYB106 may affect plant development through VLCFA biosynthesis; therefore, we propose that MIXTA-like MYBs act as global regulators of cuticular substances that regulate surface coating and developmental signaling.

Coordinate Regulation of Cuticle Development by MYB106 and WIN1/SHN1

In addition to WIN/SHN, HD-ZIP IV TFs, including HDG1, which regulates epidermal cell-specific expression via the L1-box promoter motif, are also involved in cuticle formation during plant development. These TFs regulate the *FDH* and *BDG* genes, which have an L1-box in their promoter regions (Abe et al., 2001; Wu et al., 2011). The expression of *WIN1/SHN1* is not affected in *HDG1* overexpression plants and *35S:HDG1-SRDX* plants, suggesting that *WIN1/SHN1* is not regulated by HDG1 (Wu et al., 2011). By contrast, overexpression of *CFL1*, which encodes a WW domain protein that interacts with HDG1, induced the expression of *WIN1/SHN1* (Wu et al., 2011). In this study, we found that MYB106 regulates the expression of *WIN1/SHN1*. WIN/SHNs induced the expression of *CYP86A7*, *CYP86A4*, and *BDG3* (Shi et al., 2011), which were downregulated in *MYB106-SRDX* and upregulated in *MYB106-VP16* plants. MYB106 activates the promoter of *CYP86A4*, one of the putative target genes of WIN1/SHN1, much more strongly than WIN1/SHN1 activates this promoter. There is no apparent evidence of a direct interaction between WIN1/SHN1 and MYB106; therefore, these data suggest that MYB106 and WIN1/SHN1 independently regulate *CYP86A4* expression. As described in Figure 10, we propose that MIXTA-like MYBs regulate cuticle development, epidermal cell morphogenesis, and trichome branching partly through WIN/SHNs. However, further study is still needed to clarify how and to what extent these processes are linked by the regulation of MIXTA-like MYBs, WIN/SHNs, and other TFs.

METHODS

Plant Materials and Growth Conditions

Arabidopsis thaliana ecotype Columbia-0 and *Torenia fournieri* 'Crown Violet' (Aida et al., 2000) were used as plant materials. For the *Arabidopsis MYB106* mutants (*myb106-1* and *myb106-2*), we used the T-DNA–tagged line SALK_025449 and WiscDsLoxHs 122_02H, respectively. *Arabidopsis* plants were grown at 22°C in a 16-h/8-h light/dark photoperiod. Seedlings were grown on solid agar media supplemented with Murashige and Skoog salts, 5 g/L Suc, and 0.5% MES and transferred onto soil ~15 d after germination. The growth conditions for *Torenia* flower plants and the preparation of transgenic *35S:MYB106-SRDX Torenia* were described previously (Shikata et al., 2011).

Construction of Plasmids and Plant Transformation

To construct *35S:WIN1-SRDX*, *35S:SHN3-SRDX*, *35S:MYB106-SRDX*, *35S:MYB16-SRDX*, and *35S:MYB106-VP16*, the protein-coding regions of *WIN1/SHN1*, *SHN3*, *MYB106*, and *MYB16* were amplified by PCR using the appropriate primers (see Supplemental Table 7 online) and were cloned into the *Sma*I site of p35SSRDXG and p35SVP16G as described previously (Mitsuda et al., 2006, 2011). For *35S:WIN1* and *35S:MYB106* constructs, the coding regions of *WIN1/SHN1* and *MYB106* with the stop codon were cloned into the *Sma*I site of p35SG and p35SHSPG (Oshima et al., 2011), respectively, as described previously (Mitsuda et al., 2006). To construct $MYB106_{pro}$:*MYB106-SRDX* and $MYB16_{pro}$:*MYB16-SRDX*, the 5′ upstream regions, ~3000 bp from the site of initiation of translation, of *MYB106* and *MYB16* genes were amplified by PCR and cloned into the *Asc*I-*Bam*HI site of pSRDX-NOS_entry vector (Mitsuda et al., 2007). The coding regions of *MYB106* and *MYB16* were subcloned into the *Sma*I site of the resulting plasmids. The transgene cassette was transferred into the T-DNA destination vector pBCKH by Gateway LR reaction in each case (Mitsuda et al., 2006). The 5′ upstream regions of ~3000 bp from *WIN1/SHN1* and *MYB16* were amplified by PCR and cloned into pDONRG_P4P1R (Oshima et al., 2011) by Gateway BP reaction. Preparation of the conventional entry clone of *MYB106* was previously described (Mitsuda et al., 2010).

For the construction of *WIN1*$_{pro}$:*GUS*, *MYB106*$_{pro}$:*GUS*, and *MYB16*$_{pro}$:*GUS*, the cloned promoter fragment was transferred, by Gateway LR reaction, into the T-DNA vector R4L1pDEST_GUS_BCKK, which is based on the previously described pBCKK vector (Mitsuda et al., 2006) and has *att*R4-*att*L1 Gateway cassette followed by the coding sequence of β-glucuronidase (GUS) and nopaline synthase terminator. The coding sequence of *MYB106* was transferred, by Gateway LR reaction, into pHG8_HPT, in which the *NPTII* gene is substituted for the *HPT* gene in pHellsgate8 (Helliwell and Waterhouse, 2003) to construct *35S*:*MYB106-RNAi*. The above-listed constructs and the MYB16-amiRNA construct (CSHL_070039) were transformed into *Arabidopsis* plants by the floral dip method (Clough and Bent, 1998). Transformation of *Torenia* flower was described previously (Aida and Shibata, 1995).

Scanning Electron Microscopy

The modified mold-cast technique was employed for preparing the samples (Williams et al., 1987; Jernstedt et al., 1992). Casts were coated with gold in a sputter coater (MSP-1S Magnetron Sputter; Vacuum Device). The replicas and fresh samples were examined using a scanning electron microscope (real 3D system model VE8800 and VE7800; Keyence) at an accelerating voltage of 1 or 2 kV. The area of nanoridge formation was calculated by Axio Vision 4.8 (Carl Zeiss).

Staining of Plants

Three-week-old *Arabidopsis* plants grown on Murashige and Skoog medium, mature *Arabidopsis* leaves and flowers, and *Torenia* flower leaves grown in culture pots were stained in TB following the method of Tanaka et al. (2004). The stained seedlings were washed by water and homogenized in cell lysis buffer (TOYO B-Net). Protein amounts in the extracts were measured using a Bio-Rad protein assay kit, which is based on the Bradford method (Bio-Rad). The GUS activity was detected by staining as described previously (Mitsuda et al., 2005) using 2-week-old seedling or buds. Ruthenium red staining of seed mucilage was performed as described by Penfield et al. (2001).

RNA Analysis

Total RNA was isolated from seedlings of 3-week-old T1 or T2 plants grown on hygromycin-containing medium or bud clusters of plants grown in soil. RNA was isolated by the Trizol method (Fukuda et al., 1991) or with an RNeasy plant mini kit (Qiagen) and treated with DNase I (Takara) or the RNase-Free DNase Set for use with RNeasy/QIAamp columns (Qiagen). For RT-PCR analysis, first-strand cDNA was synthesized using Ready-To-Go You-Prime first-strand beads (GE Healthcare) or a PrimeScript RT reagent kit (Takara). qRT-PCR was performed by the SYBR green method using the ABI 7300 real-time PCR system (Life Technologies) with MESA BLUE qPCR Master Mix Plus for SYBR Assay (Eurogentec) and the appropriate primers (see Supplemental Table 8 online). The cycle threshold value for each sample was automatically calculated by the software provided by the manufacturer. The relative level of transcript in each sample to the standard sample was calculated using the standard curve. The expression of each transcript was normalized against the amount of *PP2AA3* control transcripts in each sample. More than three biological replicates were included in each experiment. Results are presented as the mean ± SD. The absence of an error bar indicates that the bar falls within the symbol.

Microarray Experiments

The microarray experiments were performed using Agilent *Arabidopsis* (V3; 4x44k) microarrays (for *35S*:*MYB106-SRDX*, *35S*:*WIN1-SRDX*, and *35S*:*WIN1* plants) or *Arabidopsis* (V4; 4x44k) microarrays (for the *35S*:*MYB106-VP16* plant) according to the manufacturer's' instructions. Three or four biological replicates were tested in a one-color method. In each case, 1 μg of total RNA was used as starting material. Spot signal values were calculated by Feature Extraction version 9.1 software supplied by Agilent. We defined QC value as 1 when a spot passed the "FeatNonUnifOL" filter and as 2 when the spot further passed the "FeatPopnOL" filter and defined the detection value as 1 when a spot passed the "IsPosAndSignif" filter and as 2 when the spot further passed the "IsWellAboveBG." All signal values were divided by the median value among spots with QC = 2 followed by quantile normalization using all previously obtained microarray data to make each signal distribution the same. Spot-to-gene conversion was accomplished based on a table provided by The Arabidopsis Information Resource (ftp://ftp.Arabidopsis.org/home/tair/Microarrays/Agilent/agilent_array_elements-2010-12-20.txt). For the genes corresponding to two or more probes, the average values were used. Genes with average QC value < 1.5 in the test sample or the reference sample were excluded from subsequent analyses. Only genes with average detection value ≥ 1.5 in the reference sample were analyzed when selecting downregulated genes. The P value of each gene was calculated by Welch's *t* test. To estimate FDR, we calculated *Q*-value from P value using QVALUE software with default settings (Storey and Tibshirani, 2003) and selected downregulated genes in *35S*:*MYB106-SRDX* and *35S*:*WIN1-SRDX* plants, respectively, as the genes downregulated to <0.5 fold with P value < 0.05 (FDR was <0.05 in both experiments). Binomial test was performed using R (http://www.r-project.org/).

Transient Expression Assay

Details of the transient reporter-effector particle bombardment assay were described elsewhere (Mitsuda et al., 2011). Preparation of conventional entry clones for *WIN1*/*SHN1*, *SHN2*, *SHN3*, *MYB106*, *MYB16*, and *VAMP722* was described by Mitsuda et al. (2010). *VAMP722*, which localizes to the vacuolar membrane, was used as a negative control (Uemura et al., 2004). For effector constructs, the contents of each entry clone were introduced into the modified vectors pDEST35SHSP or pDEST35SVP16HSP derived from p35SG and p35SVP16G (Mitsuda et al., 2011) by Gateway LR reaction. For reporter constructs, 5′ upstream regions of 2000 to 3000 bp from *WIN1*/*SHN1*, *MYB106*, and *CYP86A4* were amplified by PCR using appropriate primers (see Supplemental Table 7 online) and cloned into pDONRG-P4P1R by Gateway BP reaction (Oshima et al., 2011). The contents of each plasmid were transferred into the modified vectors R4L1pDEST_LUC_HSP derived from p190LUC-NOS (Mitsuda et al., 2011) by Gateway LR reaction. Effector and reporter plasmids were cobombarded into rosette leaves of *Arabidopsis* grown in short-day (10-h-light/14-h-dark cycle) conditions. As the internal reference, a modified *Renilla* luciferase (*RLUC* or *hRLUC*; Promega) gene driven by the 35S promoter and terminated by HSP terminator (pRLHSP or phRLHSP; Nagaya et al., 2010) was also cobombarded to normalize the reporter activities.

Motif Analysis

Proteins belonging to MYB subgroup 9 were collected as follows. Proteins with significant homology to MYB106 were collected by first BLAST search against the nonredundant peptide database of the National Center for Biotechnology Information GenBank, and among them, the proteins that reversely top-hit to MYB106, MYB16, or MYB17 by second BLAST search against *Arabidopsis* in all peptide database were defined as MYB subgroup 9 proteins. Representative protein was further manually selected when multiple proteins share more than 95% amino acid sequence identity. Conserved protein motifs in the collected proteins (see Supplemental Data Set 1 online) were analyzed by Interactive SALAD analysis of the SALAD database (Mihara et al. 2008).

Accession Numbers

Sequence data from this article can be found in The Arabidopsis Information Resource under the following accession numbers: *WIN1/SHN1* (AT1G15360), *SHN2* (AT5G11190), *SHN3* (AT5G25390), *MYB106/NOK* (AT3G01140), and *MYB16* (AT5G13510). All microarray data were registered in National Center for Biotechnology Information Gene Expression Omnibus (http://www.ncbi.nlm.nih.gov/geo/) under accession number GSE31887.

Supplemental Data

The following materials are available in the online version of this article.

Supplemental Figure 1. Cuticle Permeability of *35S:MYB106-SRDX Arabidopsis* Flowers and *Torenia* Leaf.

Supplemental Figure 2. Expression and Motif Analyses Based on Public Microarray Data or Conserved Motifs among MYB Subgroup 9 Genes/Proteins, Respectively.

Supplemental Figure 3. Phenotypes Caused by Constitutive Expression of *MYB16-SRDX*.

Supplemental Figure 4. Promoter Activities of *MYB106* and *MYB16*.

Supplemental Figure 5. Promoter Activities of *MYB106* and *MYB16* in Floral Organs.

Supplemental Figure 6. Plants with Reduced Levels of MIXTA-like MYBs.

Supplemental Figure 7. Constitutive Expression of *SHN3-SRDX* Caused Reduction of Cuticular Wax with Severe Morphological Changes.

Supplemental Table 1. Frequency of Observed Phenotypes for Four Transgenes.

Supplemental Table 2. Branch Numbers of Leaf Trichomes.

Supplemental Table 3. Downregulated Gene Groups in Both *MYB106-SRDX* and *WIN1-SRDX* Plants.

Supplemental Table 4. Changes in Expression of Cuticle-Related Genes by Microarray Analysis.

Supplemental Table 5. Phenotypes of Loss-of-Function Plants.

Supplemental Table 6. Phenotypes of Gain-of-Function Plants and References.

Supplemental Table 7. Primers Used in This Study.

Supplemental Table 8. Primer Sequences for RT-PCR.

Supplemental Data Set 1. Sequences Used in Phylogenetic Analysis.

Supplemental Reference 1. Reference for Supplemental Figure 2B.

ACKNOWLEDGMENTS

We thank the ABRC for distributing seeds for T-DNA–tagged lines and the plasmid construct for amiRNA expression. We also thank Yuko Takiguchi, Sumire Fujiwara, Fumie Tobe, Naomi Ujiie, Akiko Kuwazawa, Yukie Kimura, Keiko Kigoshi, Sumiko Takahashi, and Machiko Onuki for their skillful technical assistance. This work was partly supported by the Program for Promotion of Basic and Applied Researches for Innovations in Bio-oriented Industry from the Bio-oriented Technology Research Advancement Institution, Japan (to N.M. and N.O.).

AUTHOR CONTRIBUTIONS

Y.O. performed all experiments except for microarray data and the experiments in *Torenia* flower. M.S. performed the experiments in *Torenia* flower. N.M. conducted microarray experiments. T.K. prepared some transgenic plants and recorded their phenotypes. Y.O. and N.M. designed all experiments and analyzed all data. Y.O., N.M. and M.O.-T. wrote the article. M.S., T.K., and N.O. made numerous valuable suggestions on the article. All studies were performed under the supervision of N.O. and M.O.-T.

Received February 18, 2013; revised April 23, 2013; accepted May 6, 2013; published May 24, 2013.

REFERENCES

Abe, M., Takahashi, T., and Komeda, Y. (2001). Identification of a cis-regulatory element for L1 layer-specific gene expression, which is targeted by an L1-specific homeodomain protein. Plant J. **26:** 487–494.

Aharoni, A., Dixit, S., Jetter, R., Thoenes, E., van Arkel, G., and Pereira, A. (2004). The SHINE clade of AP2 domain transcription factors activates wax biosynthesis, alters cuticle properties, and confers drought tolerance when overexpressed in *Arabidopsis*. Plant Cell **16:** 2463–2480.

Aida, R., and Shibata, M. (1995). Agrobacterium-mediated transformation of torenia (*Torenia fournieri*). Breed. Sci. **45:** 71–74.

Aida, R., Kishimoto, S., Tanaka, Y., and Shibata, M. (2000). Modification of flower color in torenia (torenia fournieri lind.) by genetic transformation. Plant Sci. **160:** 49–56.

Bach, L., Gissot, L., Marion, J., Tellier, F., Moreau, P., Satiat-Jeunemaître, B., Palauqui, J.C., Napier, J.A., and Faure, J.D. (2011). Very-long-chain fatty acids are required for cell plate formation during cytokinesis in *Arabidopsis thaliana*. J. Cell Sci. **124:** 3223–3234.

Bach, L., et al. (2008). The very-long-chain hydroxy fatty acyl-CoA dehydratase PASTICCINO2 is essential and limiting for plant development. Proc. Natl. Acad. Sci. USA **105:** 14727–14731.

Baumann, K., Perez-Rodriguez, M., Bradley, D., Venail, J., Bailey, P., Jin, H., Koes, R., Roberts, K., and Martin, C. (2007). Control of cell and petal morphogenesis by R2R3 MYB transcription factors. Development **134:** 1691–1701.

Broun, P., Poindexter, P., Osborne, E., Jiang, C.Z., and Riechmann, J.L. (2004). WIN1, a transcriptional activator of epidermal wax accumulation in *Arabidopsis*. Proc. Natl. Acad. Sci. USA **101:** 4706–4711.

Clough, S.J., and Bent, A.F. (1998). Floral dip: A simplified method for *Agrobacterium*-mediated transformation of *Arabidopsis thaliana*. Plant J. **16:** 735–743.

Cominelli, E., Sala, T., Calvi, D., Gusmaroli, G., and Tonelli, C. (2008). Over-expression of the *Arabidopsis* AtMYB41 gene alters cell expansion and leaf surface permeability. Plant J. **53:** 53–64.

Folkers, U., Berger, J., and Hülskamp, M. (1997). Cell morphogenesis of trichomes in *Arabidopsis*: Differential control of primary and secondary branching by branch initiation regulators and cell growth. Development **124:** 3779–3786.

Fukuda, Y., Ohme, M., and Shinshi, H. (1991). Gene structure and expression of a tobacco endochitinase gene in suspension-cultured tobacco cells. Plant Mol. Biol. **16:** 1–10.

Gilding, E.K., and Marks, M.D. (2010). Analysis of purified *glabra3-shapeshifter* trichomes reveals a role for *NOECK* in regulating early trichome morphogenic events. Plant J. **64:** 304–317.

Glover, B.J., Perez-Rodriguez, M., and Martin, C. (1998). Development of several epidermal cell types can be specified by the same MYB-related plant transcription factor. Development **125:** 3497–3508.

Helliwell, C., and Waterhouse, P. (2003). Constructs and methods for high-throughput gene silencing in plants. Methods **30:** 289–295.

Hiratsu, K., Matsui, K., Koyama, T., and Ohme-Takagi, M. (2003). Dominant repression of target genes by chimeric repressors that

include the EAR motif, a repression domain, in *Arabidopsis*. Plant J. **34:** 733–739.

Jaffé, F.W., Tattersall, A., and Glover, B.J. (2007). A truncated MYB transcription factor from *Antirrhinum majus* regulates epidermal cell outgrowth. J. Exp. Bot. **58:** 1515–1524.

Jakoby, M.J., Falkenhan, D., Mader, M.T., Brininstool, G., Wischnitzki, E., Platz, N., Hudson, A., Hülskamp, M., Larkin, J., and Schnittger, A. (2008). Transcriptional profiling of mature *Arabidopsis* trichomes reveals that NOECK encodes the MIXTA-like transcriptional regulator MYB106. Plant Physiol. **148:** 1583–1602.

Javelle, M., Vernoud, V., Depège-Fargeix, N., Arnould, C., Oursel, D., Domergue, F., Sarda, X., and Rogowsky, P.M. (2010). Overexpression of the epidermis-specific homeodomain-leucine zipper IV transcription factor Outer Cell Layer1 in maize identifies target genes involved in lipid metabolism and cuticle biosynthesis. Plant Physiol. **154:** 273–286.

Jenks, M.A., Tuttle, H.A., Eigenbrode, S.D., and Feldmann, K.A. (1995). Leaf epicuticular waxes of the eceriferum mutants in *Arabidopsis*. Plant Physiol. **108:** 369–377.

Jernstedt, J.A., Cutter, E.G., Gifford, E.M., and Lu, P. (1992). Angle meristem origin and development in *Selaginella martensii*. Ann. Bot. (Lond.) **69:** 351–363.

Kannangara, R., Branigan, C., Liu, Y., Penfield, T., Rao, V., Mouille, G., Höfte, H., Pauly, M., Riechmann, J.L., and Broun, P. (2007). The transcription factor WIN1/SHN1 regulates cutin biosynthesis in *Arabidopsis thaliana*. Plant Cell **19:** 1278–1294.

Li, Y., Beisson, F., Koo, A.J., Molina, I., Pollard, M., and Ohlrogge, J. (2007). Identification of acyltransferases required for cutin biosynthesis and production of cutin with suberin-like monomers. Proc. Natl. Acad. Sci. USA **104:** 18339–18344.

Li-Beisson, Y., Pollard, M., Sauveplane, V., Pinot, F., Ohlrogge, J., and Beisson, F. (2009). Nanoridges that characterize the surface morphology of flowers require the synthesis of cutin polyester. Proc. Natl. Acad. Sci. USA **106:** 22008–22013.

Lippold, F., Sanchez, D.H., Musialak, M., Schlereth, A., Scheible, W.R., Hincha, D.K., and Udvardi, M.K. (2009). AtMyb41 regulates transcriptional and metabolic responses to osmotic stress in *Arabidopsis*. Plant Physiol. **149:** 1761–1772.

Lolle, S.J., Berlyn, G.P., Engstrom, E.M., Krolikowski, K.A., Reiter, W.D., and Pruitt, R.E. (1997). Developmental regulation of cell interactions in the *Arabidopsis* fiddlehead-1 mutant: A role for the epidermal cell wall and cuticle. Dev. Biol. **189:** 311–321.

Lolle, S.J., Cheung, A.Y., and Sussex, I.M. (1992). Fiddlehead: An *Arabidopsis* mutant constitutively expressing an organ fusion program that involves interactions between epidermal cells. Dev. Biol. **152:** 383–392.

Lü, S., Zhao, H., Parsons, E.P., Xu, C., Kosma, D.K., Xu, X., Chao, D., Lohrey, G., Bangarusamy, D.K., Wang, G., Bressan, R.A., and Jenks, M.A. (2011). The glossyhead1 allele of ACC1 reveals a principal role for multidomain acetyl-coenzyme A carboxylase in the biosynthesis of cuticular waxes by *Arabidopsis*. Plant Physiol. **157:** 1079–1092.

Mihara, M., Itoh, T., and Izawa, T. (2008). In silico identification of short nucleotide sequences associated with gene expression of pollen development in rice. Plant Cell Physiol. **49:** 1451–1464.

Mitsuda, N., Hiratsu, K., Todaka, D., Nakashima, K., Yamaguchi-Shinozaki, K., and Ohme-Takagi, M. (2006). Efficient production of male and female sterile plants by expression of a chimeric repressor in *Arabidopsis* and rice. Plant Biotechnol. J. **4:** 325–332.

Mitsuda, N., Ikeda, M., Takada, S., Takiguchi, Y., Kondou, Y., Yoshizumi, T., Fujita, M., Shinozaki, K., Matsui, M., and Ohme-Takagi, M. (2010). Efficient yeast one-/two-hybrid screening using a library composed only of transcription factors in *Arabidopsis thaliana*. Plant Cell Physiol. **51:** 2145–2151.

Mitsuda, N., Iwase, A., Yamamoto, H., Yoshida, M., Seki, M., Shinozaki, K., and Ohme-Takagi, M. (2007). NAC transcription factors, NST1 and NST3, are key regulators of the formation of secondary walls in woody tissues of *Arabidopsis*. Plant Cell **19:** 270–280.

Mitsuda, N., Matsui, K., Ikeda, M., Nakata, M., Oshima, Y., Nagatoshi, Y., and Ohme-Takagi, M. (2011). CRES-T, an effective gene silencing system utilizing chimeric repressors. Methods Mol. Biol. **754:** 87–105.

Mitsuda, N., Seki, M., Shinozaki, K., and Ohme-Takagi, M. (2005). The NAC transcription factors NST1 and NST2 of *Arabidopsis* regulate secondary wall thickenings and are required for anther dehiscence. Plant Cell **17:** 2993–3006.

Nagaya, S., Kawamura, K., Shinmyo, A., and Kato, K. (2010). The HSP terminator of *Arabidopsis thaliana* increases gene expression in plant cells. Plant Cell Physiol. **51:** 328–332.

Noda, K., Glover, B.J., Linstead, P., and Martin, C. (1994). Flower colour intensity depends on specialized cell shape controlled by a Myb-related transcription factor. Nature **369:** 661–664.

Oshima, Y., Mitsuda, N., Nakata, M., Nakagawa, T., Nagaya, S., Kato, K., and Ohme-Takagi, M. (2011). Novel vector systems to accelerate functional analysis of transcription factors using chimeric repressor gene-silencing technology (CRES-T). Plant Biotechnol. **28:** 201–210.

Panikashvili, D., Shi, J.X., Schreiber, L., and Aharoni, A. (2009). The *Arabidopsis* DCR encoding a soluble BAHD acyltransferase is required for cutin polyester formation and seed hydration properties. Plant Physiol. **151:** 1773–1789.

Pastore, J.J., Limpuangthip, A., Yamaguchi, N., Wu, M.F., Sang, Y., Han, S.K., Malaspina, L., Chavdaroff, N., Yamaguchi, A., and Wagner, D. (2011). LATE MERISTEM IDENTITY2 acts together with LEAFY to activate APETALA1. Development **138:** 3189–3198.

Penfield, S., Meissner, R.C., Shoue, D.A., Carpita, N.C., and Bevan, M.W. (2001). MYB61 is required for mucilage deposition and extrusion in the *Arabidopsis* seed coat. Plant Cell **13:** 2777–2791.

Perez-Rodriguez, M., Jaffe, F.W., Butelli, E., Glover, B.J., and Martin, C. (2005). Development of three different cell types is associated with the activity of a specific MYB transcription factor in the ventral petal of *Antirrhinum majus* flowers. Development **132:** 359–370.

Pruitt, R.E., Vielle-Calzada, J.P., Ploense, S.E., Grossniklaus, U., and Lolle, S.J. (2000). FIDDLEHEAD, a gene required to suppress epidermal cell interactions in *Arabidopsis*, encodes a putative lipid biosynthetic enzyme. Proc. Natl. Acad. Sci. USA **97:** 1311–1316.

Raffaele, S., Vailleau, F., Léger, A., Joubès, J., Miersch, O., Huard, C., Blée, E., Mongrand, S., Domergue, F., and Roby, D. (2008). A MYB transcription factor regulates very-long-chain fatty acid biosynthesis for activation of the hypersensitive cell death response in *Arabidopsis*. Plant Cell **20:** 752–767.

Rani, S.H., Krishna, T.H., Saha, S., Negi, A.S., and Rajasekharan, R. (2010). Defective in cuticular ridges (DCR) of *Arabidopsis thaliana*, a gene associated with surface cutin formation, encodes a soluble diacylglycerol acyltransferase. J. Biol. Chem. **285:** 38337–38347.

Roudier, F., et al. (2010). Very-long-chain fatty acids are involved in polar auxin transport and developmental patterning in *Arabidopsis*. Plant Cell **22:** 364–375.

Schmid, M., Davison, T.S., Henz, S.R., Pape, U.J., Demar, M., Vingron, M., Schölkopf, B., Weigel, D., and Lohmann, J.U. (2005). A gene expression map of *Arabidopsis thaliana* development. Nat. Genet. **37:** 501–506.

Schnurr, J., Shockey, J., and Browse, J. (2004). The acyl-CoA synthetase encoded by LACS2 is essential for normal cuticle development in *Arabidopsis*. Plant Cell **16:** 629–642.

Seo, P.J., Lee, S.B., Suh, M.C., Park, M.J., Go, Y.S., and Park, C.M. (2011). The MYB96 transcription factor regulates cuticular wax

biosynthesis under drought conditions in *Arabidopsis*. Plant Cell **23:** 1138–1152.

Shi, J.X., Malitsky, S., De Oliveira, S., Branigan, C., Franke, R.B., Schreiber, L., and Aharoni, A. (2011). SHINE transcription factors act redundantly to pattern the archetypal surface of *Arabidopsis* flower organs. PLoS Genet. **7:** e1001388.

Shikata, M., Narumi, T., Yamaguchi, H., Sasaki, K., Aida, R., Oshima, Y., Takiguchi, Y., Ohme-Takagi, M., Mitsuda, N., and Ohtsubo, N. (2011). Efficient production of novel floral traits in torenia by collective transformation with chimeric repressors of *Arabidopsis* transcription factors. Plant Biotechnol. **28:** 189–199.

Storey, J.D., and Tibshirani, R. (2003). Statistical significance for genomewide studies. Proc. Natl. Acad. Sci. USA **100:** 9440–9445.

Stracke, R., Werber, M., and Weisshaar, B. (2001). The R2R3-MYB gene family in *Arabidopsis thaliana*. Curr. Opin. Plant Biol. **4:** 447–456.

Suh, M.C., Samuels, A.L., Jetter, R., Kunst, L., Pollard, M., Ohlrogge, J., and Beisson, F. (2005). Cuticular lipid composition, surface structure, and gene expression in *Arabidopsis* stem epidermis. Plant Physiol. **139:** 1649–1665.

Taketa, S., et al. (2008). Barley grain with adhering hulls is controlled by an ERF family transcription factor gene regulating a lipid biosynthesis pathway. Proc. Natl. Acad. Sci. USA **105:** 4062–4067.

Tanaka, T., Tanaka, H., Machida, C., Watanabe, M., and Machida, Y. (2004). A new method for rapid visualization of defects in leaf cuticle reveals five intrinsic patterns of surface defects in *Arabidopsis*. Plant J. **37:** 139–146.

Todd, J., Post-Beittenmiller, D., and Jaworski, J.G. (1999). KCS1 encodes a fatty acid elongase 3-ketoacyl-CoA synthase affecting wax biosynthesis in *Arabidopsis thaliana*. Plant J. **17:** 119–130.

Uemura, T., Ueda, T., Ohniwa, R.L., Nakano, A., Takeyasu, K., and Sato, M.H. (2004). Systematic analysis of SNARE molecules in *Arabidopsis*: Dissection of the post-Golgi network in plant cells. Cell Struct. Funct. **29:** 49–65.

Wellesen, K., Durst, F., Pinot, F., Benveniste, I., Nettesheim, K., Wisman, E., Steiner-Lange, S., Saedler, H., and Yephremov, A. (2001). Functional analysis of the LACERATA gene of *Arabidopsis* provides evidence for different roles of fatty acid omega -hydroxylation in development. Proc. Natl. Acad. Sci. USA **98:** 9694–9699.

Williams, M.H., Vesk, M., and Mullins, M.G. (1987). Tissue preparation for scanning electron microscopy of fruit surfaces: Comparison of fresh and cryopreserved specimens and replicas of banana peel. Microsc. Acta **18:** 27–31.

Wu, R., Li, S., He, S., Wassmann, F., Yu, C., Qin, G., Schreiber, L., Qu, L.J., and Gu, H. (2011). CFL1, a WW domain protein, regulates cuticle development by modulating the function of HDG1, a class IV homeodomain transcription factor, in rice and *Arabidopsis*. Plant Cell **23:** 3392–3411.

Yephremov, A., Wisman, E., Huijser, P., Huijser, C., Wellesen, K., and Saedler, H. (1999). Characterization of the FIDDLEHEAD gene of *Arabidopsis* reveals a link between adhesion response and cell differentiation in the epidermis. Plant Cell **11:** 2187–2201.